

New X-ray Selected Pre-Main Sequence Members of the Serpens Molecular Cloud

Isa Oliveira^{1,4}, Margriet van der Laan², & Joanna M. Brown³

ABSTRACT

The study of young stars no longer surrounded by disks can greatly add to our understanding of how protoplanetary disks evolve and planets form. We have used VLT/FLAMES optical spectroscopy to confirm the youth and membership of 19 new young diskless stars in the Serpens Molecular Cloud, identified at X-ray wavelengths. Spectral types, effective temperatures and stellar luminosities were determined using the optical spectra and optical/near-IR photometry. Stellar masses and ages were derived based on PMS evolutionary tracks. The results yield remarkable similarities for age and mass distribution between the diskless and disk-bearing stellar populations in Serpens. We discuss the important implications these similarities may have on the standard picture of disk evolution.

Subject headings: ISM: individual objects (Serpens) – stars: pre-main sequence – circumstellar matter

1. Introduction

The manner in which protoplanetary disks evolve and, potentially, form planets is one of the most exciting subjects of research in astrophysics in the last decade. Through multi-wavelength observations, combined with a growing number of models and theories, many complex processes have been found to play a role in explaining how planets could possibly form from the small dust and gas initially present in those disks. It is not yet clear exactly under which circumstances the different processes are determinant. However, it is clear that the study of protoplanetary disks alone is unlikely to lead to a full picture of disk evolution.

¹McDonald Observatory, The University of Texas at Austin, 1 University Station, C1402, Austin, TX 78712, USA; email: oliveira@astro.as.utexas.edu

²Leiden Observatory, Leiden University, P.O. Box 9513, 2300 RA Leiden, The Netherlands

³Harvard-Smithsonian Center for Astrophysics, 60 Garden St., MS 78, Cambridge, MA 02138, USA

⁴Harlan J. Smith Postdoctoral Fellow

A powerful way to learn more about disks is to study young stars that no longer are surrounded by them. It is believed that all stars are born harboring circumstellar disks, through conservation of angular momentum during the star formation process. Observations have shown that not all disks have the same lifetime, but that they vary between approximately 1 and 10 Myr, with about 50% of dusty disks disappearing within 3 Myr (e.g. Haisch et al. 2001; Hernández et al. 2008). Differences between young stars of the same age with and without disks could yield a greater understanding of the processes that affect disk evolution, and eventually allow time for planets to form.

The difficulty in studying young stars without disks lies in identifying them. Young stars are most commonly found on the basis of their colors, which takes into account the presence of the dusty disk emission, prominent in the infra-red (IR) region of the system (star+disk) spectrum. If a young star is no longer surrounded by a disk, its optical-IR colors are indistinguishable from fore-/background stars observed in the same direction as the star-forming region to which it belongs. With broad-band optical/IR photometric studies, it can be difficult to identify candidate diskless young stars.

The picture changes considerably when studying a region at X-ray wavelengths. In this short-wavelength regime, young stars are very active whether or not a disk is still present (e.g. Preibisch et al. 2005; Feigelson et al. 2007). Indeed, X-ray emission has been often used to identify young stellar objects in the literature (e.g. Feigelson & Kriss 1981; Walter & Kuhl 1981; Feigelson & Montmerle 1999; Getman et al. 2005; Padgett et al. 2006; Güdel et al. 2007; Winston et al. 2007; Telleschi et al. 2007). Confirmation of their young stellar nature, however, is necessary through other means, the most powerful of which being optical spectroscopy (e.g. Walter et al. 1988; Scelsi et al. 2008).

The Serpens Molecular Cloud is a young star-forming region (~ 2 Myr, Oliveira et al. 2013). VLBI measurements by Dzib et al. (2010) of EC95 in The Serpens Core indicate it at a distance of 415 pc. Given the size of the cloud, it is reasonable to assume a distance of 415 ± 15 pc for its entirety. The young stellar population still surrounded by disks in Serpens beyond its core has been uncovered in the infrared by the *Spitzer Space Telescope* Legacy Program ‘c2d’ (Harvey et al. 2006, 2007a,b). Unlike the Serpens Core, which has been well studied in a variety of wavelengths (e.g. Winston et al. 2007, 2009, 2010), nothing was known about the diskless young stellar population of Serpens beyond its core until it was observed with *XMM-Newton* (Brown et al., in prep). Two *XMM-Newton* pointings cover about 2/3 of the Serpens area observed by the c2d, and dozens of objects were identified by Brown et al. as young diskless star candidates, for which confirmation is still necessary.

In this paper we report on an optical multi-object spectroscopic survey designed to confirm the youth and membership of those newly-discovered young diskless star candidates

discovered in Serpens with *XMM-Newton*. Section 2 describes the VLT/FLAMES observations and data reduction. The data are analysed in Section 3, where spectral types, stellar temperatures and luminosities are determined. Spectral energy distributions (SEDs) are constructed with the addition of optical, near- and mid-IR photometry from the literature. Then, the objects are placed in a HR diagram overlaid with pre-main sequence evolutionary tracks, from which individual ages and masses are derived. In Section 4, the bona-fide diskless young stellar population of Serpens is discussed and contextualized with respect to the disk-bearing population (Oliveira et al. 2009, 2010, 2013). Finally, we present our conclusions in Section 5.

2. Observations and Data Reduction

The spectroscopic data were obtained using the Fibre Large Array Multi-Element Spectrograph (FLAMES) on the 8.2m UT2 (Kueyen) telescope of ESO, in Paranal, Chile, in service mode in June, 2009. FLAMES consists of three components: a Fibre Positioner (OzPoz), a medium-high resolution optical spectrograph GIRAFFE, and a link to the instrument UVES. The data used in this work consist of two observing blocks from FLAMES/GIRAFFE using the MEDUSA fibers. This setting allows for up to 132 fibers of 1.2'' aperture in the 25' diameter field of view of the instrument. The wavelength range chosen, 6437–7183 Å, offers a spectral resolution of 0.8 Å and covers temperature-sensitive features that allow spectral classification.

The two observed fields (AO5 and AO6) were centered on the *XMM-Newton* observations. An input list of the young stellar candidates coordinates was provided based on X-ray detections from Brown et al. (in prep.). AO5, observed by *XMM-Newton* on 2007-04-15 in program 0402820101, was centered at 277.254625 +0.49727778, and AO6, observed 2008-04-16 in XMM program 0503240201, was centered at 277.34775 +0.8228333. *XMM-Newton* has a slightly larger aperture than FLAMES at 30' versus 25' so candidates on the edges of the XMM fields could not be observed. All X-ray sources, regardless of optical or infrared characteristics were considered for follow-up. Preference was given to targets with optical counterparts which are not part of the *Spitzer* disk sample in the same region (Harvey et al. 2006, 2007a,b) and had no previously known spectral information. Fiber placement was optimized using the FPOSS Fibre configuration program of FLAMES, which permitted observation of most candidates. However, some candidates could not be simultaneously observed and had to be dropped. Unused fibers were placed on 'blank' positions of the sky for sky subtraction. To maximize dynamic range, fields were observed using multiple 2000 second exposures. Field AO5 had 5 such exposures and field AO6 had 4. A summary

of the observational details can be found in Table 1.

Data reduction was performed within the ESO reduction pipeline GASGANO. The pipeline performs frame correction for detector defects, fiber localization and tracing, flat-fielding and fiber transmission, correction of scattered light and wavelength calibration. The science spectra were extracted within IDL after wavelength calibration. For each observed field, all sky spectra were combined with a 2σ clipping in order to exclude cosmic rays or any other artifacts. This combined sky spectrum was then subtracted from the science spectra to remove sky lines. Since each field was observed more than once (see Table 1), all observed spectra of the same object are combined, also with a 2σ clipping, leading to the final spectrum of each object. Figure 1 shows a representative sample of the spectra of the objects in this sample.

The final dataset consists of 86 observed objects, being 26 from field AO5 and 60 from field AO6 (details in Tables 2 and 3, respectively). However, 61 of these objects turned out to be much too faint and their spectra are underexposed, without enough signal-to-noise ratio (S/N) to show any of the features necessary for spectral classification (S/N $\gtrsim 10$ per pixel). These objects are marked as low S/N in Tables 2 and 3 and are left out of further analysis.

3. Data Analysis

The positions of the 25 objects analyzed are shown in Figure 2. The 7 objects in field AO5 are shown in blue, while the 18 objects in AO6 are in red. The Serpens members with disks, as observed with *Spitzer* by Oliveira et al. (2010) are shown in gray for comparison.

It is worth noting that the spectra presented here cover the H α line, an indicator of mass accretion onto the star (White & Basri 2003; Muzerolle et al. 2003; Natta et al. 2004), and the Li I absorption line, often used as a general indicator of stellar youth. Lithium can be depleted in low-mass stars (late-K and M-types) due to fusion in the stellar interior. Evolutionary models predict depletion to start at $\sim 10 - 20$ Myr and proceed quickly. Stars more massive than $\sim 1 M_{\odot}$ develop radiative cores, limiting mixing to the center, which retards depletion (Randich et al. 2001; Hartmann 2003). Due to variations in S/N, Li I could not be detected in all of the spectra presented here. The detection criterion adopted is an equivalent width greater than 0.1 \AA . The presence (in emission or absorption) or absence of these lines, as well as the presence of IR-excess in those sources, are indicated in Table 4.

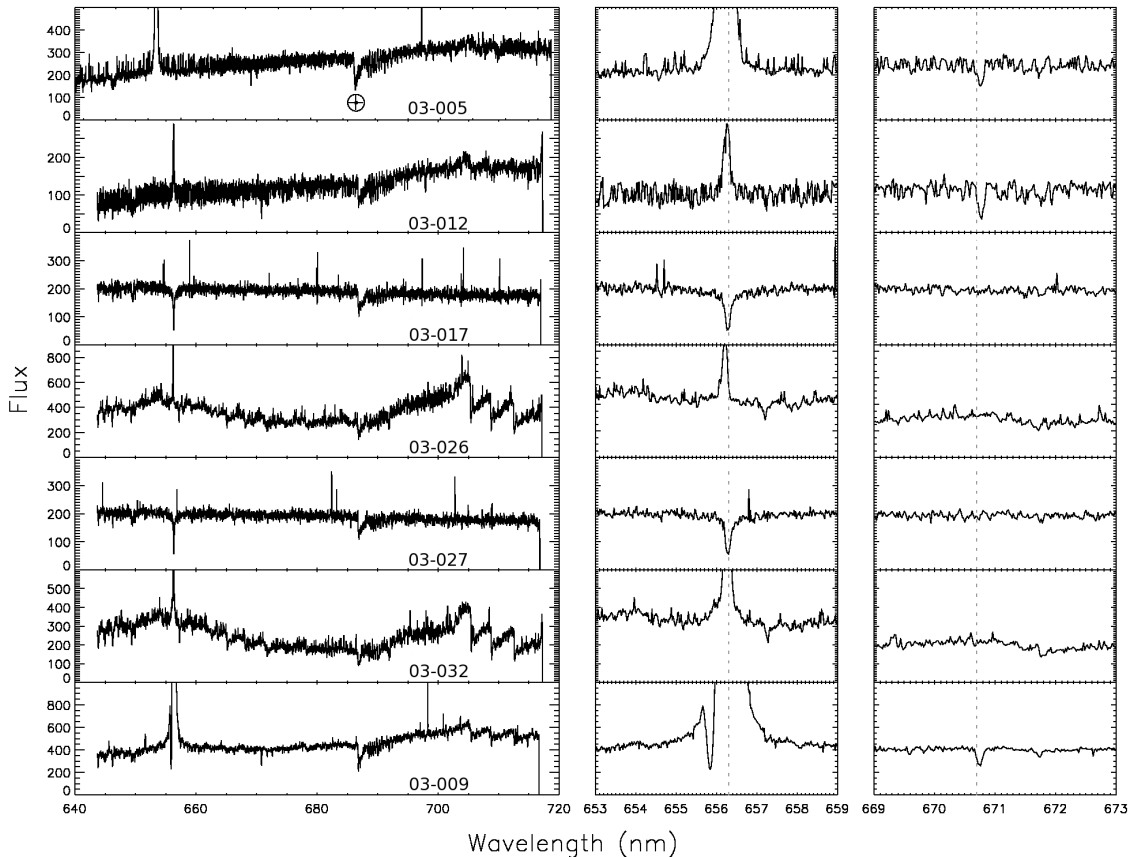


Fig. 1.— Selected spectra of a representative sample of the observed objects in this sample. The left panel shows the entire wavelength coverage with its correspondent object ID. The most prominent features seen in late-type stars are the titanium oxide (TiO) absorption bands at 7050 – 7150 Å. The middle panel shows the H α region, and the right panel shows the Li I line.

3.1. Spectral Types

Spectral classification of the 25 objects is performed by comparing each spectrum to a library of standards, following Oliveira et al. (2009) and Mortier et al. (2011). The routine used here classifies the optical spectra by a direct comparison with the grid of standards from EXPORT (Mora et al. 2001) and one from Montes et al. (1997). In this routine the science spectra are first normalized to the continuum and then over-plotted on the normalized standards of different spectral types. A χ^2 minimization is performed to find the best fit amongst all spectral types, followed by a visual inspection of each object. This method yields an accuracy of a half spectral class given the range of standard spectra available. A larger

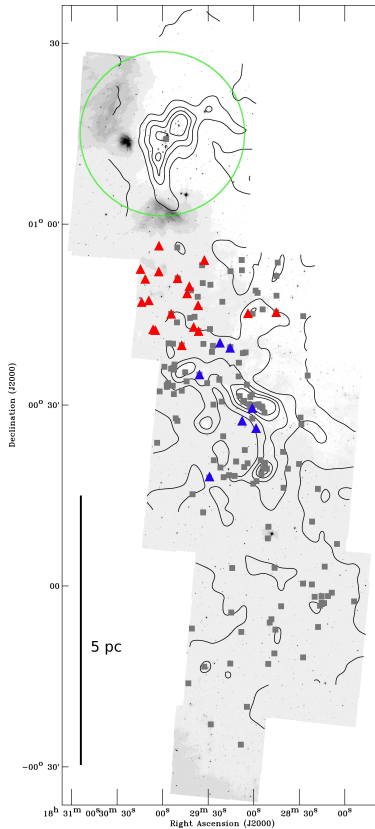


Fig. 2.— Observed objects over-plotted on the $8.0 \mu\text{m}$ IRAC 4 map of the Serpens molecular cloud. Young star candidates from this work are shown as red (field AO6) and blue (field AO5) triangles. Gray squares show the positions of the young stars with disks from Oliveira et al. (2010) for comparison. The contours (5, 10, 15, 20 and 25 mag) of visual extinction are derived from the c2d extinction maps (Evans et al. 2007). The large green circle indicates the Serpens Core.

uncertainty is found for the spectra with lower S/N. The distribution of spectral types from this work is shown in Figure 3, while the results for individual stars can be found in Table 4.

Similar to the distribution of spectral types of the young stars with disks (Oliveira et al. 2009), the majority of stars in this sample are of late K and M spectral types, with only a few being earlier G-types.

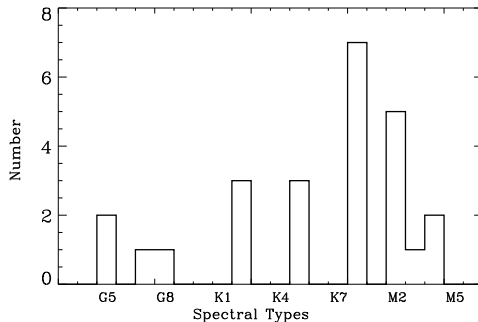


Fig. 3.— Distribution of spectral types of young diskless star candidates in Serpens based on the classification scheme described in section 3.1.

3.2. Stellar Temperatures

Effective temperatures (T_{eff}) for the individual objects were determined using calibrations that relate them to spectral types. For stars of type earlier than M0, the relationship established by Kenyon & Hartmann (1995) is used, while for stars of later type the relationship from Luhman et al. (2003) was adopted. The errors in T_{eff} come directly from the errors in the spectral types (Section 3.1). The results can be found in Table 5.

3.3. Stellar Luminosities

Stellar luminosities are calculated by integrating the NEXTGEN model atmosphere (Hauschildt et al. 1999; Allard et al. 2000) corresponding to each object’s spectral type, scaled to its dereddened optical and near-IR photometry and assuming a distance 415 ± 15 pc (Dzib et al. 2010). Optical R- and Z-band photometry for this region is available in the literature (Spezzi et al. 2010), although not all objects have been detected due to the high extinction towards some regions of the cloud. When optical photometry was not available, the Two Micron All Sky Survey (2MASS) photometry was used to scale the model atmospheres. Similar methods for luminosity estimates have been broadly used in the literature (Kenyon & Hartmann 1995; van den Ancker et al. 1997; Alcalá et al. 2008; Merín et al. 2008; Oliveira et al. 2009, 2013; Mortier et al. 2011). The uncertainties in luminosity are derived from the errors in the distance and on the extinction (± 2 mag). The results can be found in Table 5.

Objects 03-009 and 03-027 have no available optical or near-IR photometry and therefore are left out of any further analysis. All the following discussion concerns the remaining 23

objects.

3.4. Spectral Energy Distributions

The constructed spectral energy distributions (SEDs) for the 23 young diskless star candidates are shown in Figure 4 and 5. Besides the corresponding NEXTGEN model atmosphere (solid black line) and available optical/near-IR photometry from the literature, as discussed in the previous section, *Spitzer* mid-IR photometry is added where available. The IRAC (at 3.6, 4.5, 5.8 and 8.0 μm) and MIPS (at 24 μm) band fluxes were published by Harvey et al. (2006, 2007a,b). In the figures, the crosses indicate the observed photometry, while the blue filled circles show the extinction corrected photometry. Individual extinction values were derived to best match the stellar photosphere, using the extinction law of Weingartner & Draine (2001).

3.5. Stellar Ages & Masses

Once T_{eff} and L_{star} are known, it is possible to place the objects in a HR diagram (Figure 6). With the aid of pre-main sequence (PMS) evolutionary tracks, ages and masses can be derived for young stars by comparing each object’s position to the isochrones and mass tracks of a particular model. Due to the physics and calibration of each model, the models of Baraffe et al. (2001) are used for stars less massive than $1.4 M_{\odot}$, while more massive stars are compared to the models of Siess et al. (2000). The results are displayed in Table 5.

Due to the relatively old ages ($> 2 \times 10^7$ yr) derived for objects 02-005, 02-008, 02-025 and 02-039, it is unclear whether they indeed belong to the cloud, given the uncertainty of PMS evolutionary models. It is worth noting that the spectra of objects 02-005 and 02-025 do not show Li I, while the line is seen in the spectra of 02-008 and 02-039. At this point it is difficult to confirm membership and these four objects are left out of the further discussion. The remaining 19 objects are confirmed new members of Serpens.

3.5.1. Infrared Excess

It can be seen from Figures 4 and 5 that 6 out of 19 new confirmed members of Serpens (03-005, 02-007, 02-028, 02-037, 02-057 and 02-072) show some IR-excess. Objects 02-007 and 02-028 show excess emission throughout the *Spitzer* bands. This is considered weak IR-excess for being lower than the median excess for objects in Taurus (Furlan et al. 2006), the

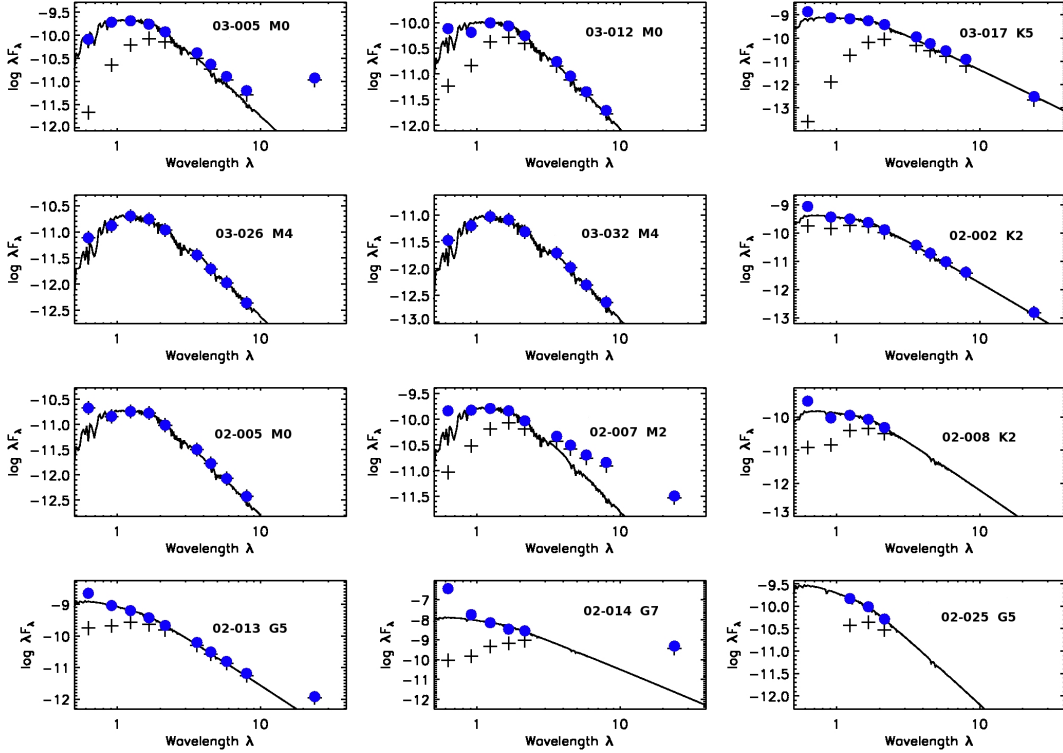


Fig. 4.— Spectral energy distributions of the new young diskless population in Serpens. Each SED has the corresponding object ID (as in Tables 2 and 3). The solid black line indicates the NextGen Atmosphere model for the corresponding spectral type of each object, also shown in the plot. Plus signs indicate the observed photometry while solid blue circles denote the dereddened photometry. No SEDs are shown for the objects without photometric data (objects 03-009 and 03-027).

prototype for full disks. The other four objects have SEDs indicative of cold or transitional disks, where no excess is seen in the near- to mid-IR, and a more substantial excess is present at mid- to far-IR. Object 03-005 was indeed previously confirmed as a cold disk with *Spitzer* IRS spectra (Merín et al. 2010). Objects 02-037, 02-057 and 02-072 are new cold disk candidates. None of the four older objects, not yet confirmed to be members of the cloud, show any IR excess.

Following White & Basri (2003), we identify $H\alpha$ emission in Table 4 as strong (full width at 10% of peak intensity higher than 270 km s^{-1}) or weak ($H\alpha$ 10% $\leq 270 \text{ km s}^{-1}$). In addition, in Table 4 ‘A’ indicates that $H\alpha$ is seen in absorption. Three out of the 19 new members show strong emission of the $H\alpha$ line. These objects (03-005, 02-037 and 02-072)

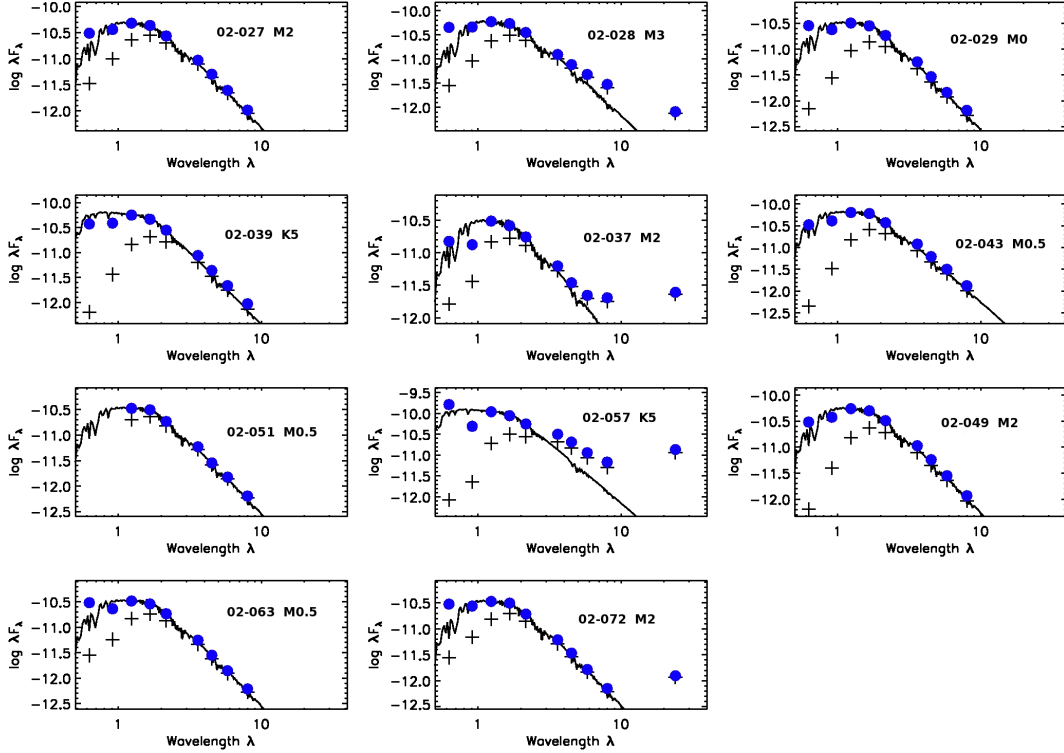


Fig. 5.— SEDs, continued.

also show IR excess, indicating that disks are still present. None of the confirmed diskless sources show strong $H\alpha$ emission, albeit some do show weak $H\alpha$ emission, which can be attributed to chromospheric activity (White & Basri 2003).

This way, 86 stars were observed by FLAMES but only 25 objects are bright enough for spectral classification. Out of these 25 objects analyzed, 19 are confirmed new members of Serpens, while the other 6 could not be confirmed or rejected at this point. Out of the new confirmed members of the cloud, 2/3 are show to be diskless, while the other 1/3 show IR-excess weaker than the median of Taurus.

4. Discussion

The most straightforward explanation for why the disks around these newly confirmed young stars have already dissipated would be that these stars are systematically a few Myr

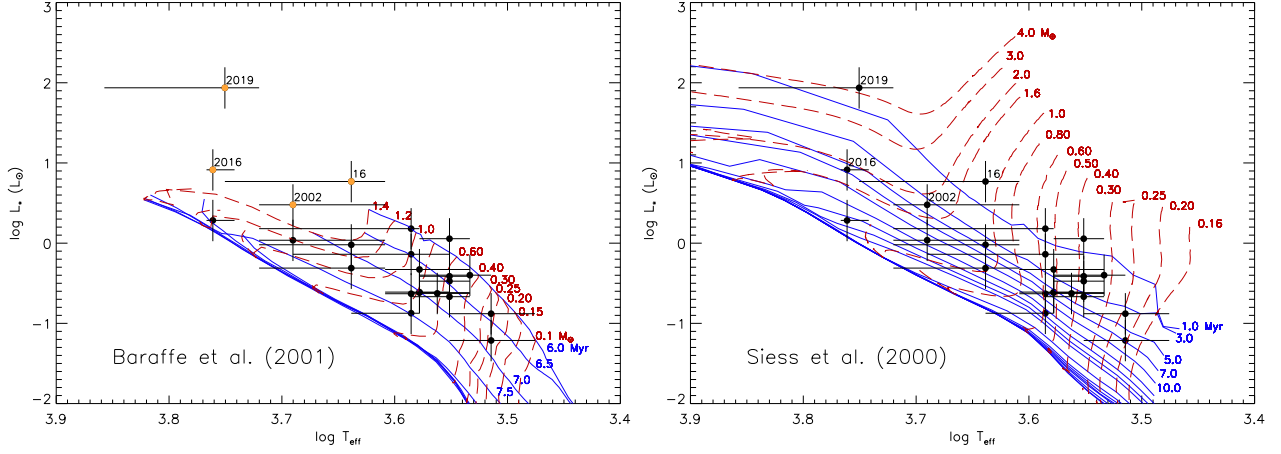


Fig. 6.— HR diagrams overlaid with the pre-main sequence evolutionary models of Baraffe et al. (2001), left, and Siess et al. (2000), right.

older than the stars with disks in the same area of Serpens (Oliveira et al. 2013). The higher ages would be sufficient for their disks to have evolved and dissipated. This could be the case for the older objects 02-005, 02-008, 02-025 and 02-039, if these objects indeed belong to the cloud. Another possibility would be that these diskless stars are consistently more massive than the disk-bearing stars in the same area of Serpens of the same age. It has been shown that disk lifetimes are related to the host star mass, with higher mass stars having disks that dissipated faster (Carpenter et al. 2006; Kennedy & Kenyon 2009).

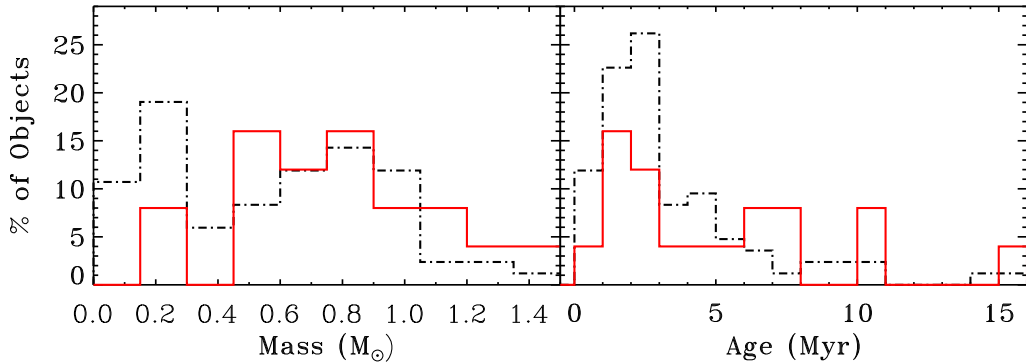


Fig. 7.— Distribution of masses and ages of the new young objects confirmed in Serpens (solid red lines). The distribution of the previously known YOSs in Serpens (Oliveira et al. 2013) is shown for comparison (dot-dashed black lines).

Figure 7 shows the mass and age distributions for our sample of newly-confirmed members of Serpens (solid red lines), and those for the disk-bearing young stars in the same region (dot-dashed black lines; Oliveira et al. 2013). It is immediately clear that, although not perfect copies of each other (KS statistical tests show that the hypothesis that they are drawn from different distributions is not supported, with probabilities $P = 24\%$ and 10% for the distributions of ages and masses, respectively), the distributions of both stellar ages and masses of diskless young stars have the same spread, and even the same peak locations, as those of disk-bearing stars in the same region. Once again it is important to note that only the confirmed new members are taken into consideration here. If the 4 older stars (Section 3.5) are indeed members of the cloud, the statistical significance would change for the age distribution ($P=0.09$ and 0.4 for the distributions of ages and masses, respectively). However, it is true that the bulk of this new population is not consistently shifted towards larger ages.

Although we acknowledge that the sample studied here does not necessarily represent the entire population of diskless young stars in Serpens, the similarity of the distributions suggest that ages and stellar masses are not absolute drivers of disk evolution. Other parameters must play an important role, such that stars of similar age and mass end up having such different disks (or lack thereof). That is not to say that either parameter is not important for disk evolution: the big picture remains that disks evolve with time and, statistically, older stars have more evolved (or no) disks compared to young stars. However, a complete theory of protoplanetary disk evolution must take into account that stars of similar age and in the same environment do present an large variety in disk structures (e.g Furlan et al. 2006; Fang et al. 2009; Oliveira et al. 2010, 2013; Sicilia-Aguilar et al. 2011) or no disks at all.

Similar results were seen by Feigelson & Montmerle (1999). From a reliable X-ray sample from the ROSAT satellite, stars were characterized spectroscopically and placed in HR diagrams. They report that in the Chamaeleon I and Taurus-Auriga star-forming regions, no significant differences are seen in the age distributions of disk-bearing (class II) and diskless (class III) stars. In that work, the authors discuss two immediate consequences of these results: (i) an underestimate of cloud star formation rates for samples dominated by class II stars; and (ii) that the high numbers of class III stars in young regions imply that many (at least 1/2 of low-mass stars in Chamaeleon I) lose their disks within 1 Myr. In that work, the authors already argued that there is no preferred disk lifetime, since disk-bearing and diskless stars coexist along the Hayashi track.

More recently, aided by *Chandra* observations and optical spectroscopy, Winston et al. (2009, 2010) showed very similar age distributions for class II and class III stars in the Serpens Core and NGC1333. They argued that young stellar populations with and without

disks show indistinguishable spatial and age distributions, suggesting that class III stars are not typically older stars, but rather stars that lost their disks quicker.

In addition, Cieza et al. (2007) and Beccari et al. (2010) have studied the differences between classical T Tauri stars (CTTS, young stars actively accreting material from their disks) and weak-line T Tauri stars (WTTS, young stars that show no signs of accretion). Correspondingly, both studies find no significant difference in the age distributions of CTTS and WTTS. However, it is important to note that not all WTTS are bona-fide class III objects. Many WTTS have disks (even thick disks) but that for some reason are no longer accreting material onto their host stars. Therefore, what these results show is that there is no significant difference in the age distribution of stars that are actively accreting from their disks and stars that are not.

Several different processes actively being studied could possibly be responsible for the fast dissipation of some disks, while others last many Myr. For instance, a relationship between the disk mass (from 1.3 mm observations with the Submillimeter Array) and stellar mass has been shown to be real for a complete disk sample in Taurus by Andrews et al. (2013). If confirmed for other complete and unbiased samples, this result puts strong constraints on theories for disk evolution and planet formation. The stellar mass would be decisive on how much material is available in disks for planets to form from.

Another interesting process that could be decisive on disk evolution timescales is photoevaporation. Theoretical calculations predict that energetic UV and X-ray photons emitted by the central star could heat the surface of the disk and cause pressure-driven hydrodynamic mass outflows from the disk (Hollenbach et al. 2000; Clarke et al. 2001; Alexander et al. 2006a,b; Ercolano et al. 2009; Gorti et al. 2009; Owen et al. 2010). Coupled with the disk viscous evolution, disks could be dispersed in $\sim 10^6$ Myr. Observational confirmation of photoevaporation is an active field that has already produced some interesting results (e.g. Pascucci & Sterzik 2009; Pascucci et al. 2012).

Just as exciting, and perhaps even more observationally challenging, is the effect of multiplicity on disk evolution. Since the majority of low-mass stars form in multiple systems, binary companions can affect disk evolution directly. Kraus et al. (2012) showed these effects for the first time on a complete sample in Taurus-Auriga. They found that tidal influence of a close binary ($\lesssim 40$ AU) accelerates significantly disk dispersal, with disks being completely dissipated within 1 Myr for $\sim 2/3$ of close binaries. The same is true for only a small fraction of wide binaries and single stars ($\sim 10 - 20\%$) whose disks are dispersed within 2–3 Myr. These exciting results must be confirmed with similar observations of complete samples of young stars in different star-forming regions, of different mean ages and environments.

5. Conclusions

We have confirmed, for the first time, a significant population of young diskless stars discovered at X-ray wavelengths that are members of the Serpens Molecular Cloud.

We have determined spectral types, effective temperatures and luminosities using optical spectroscopy from VLT/FLAMES and optical/near-IR photometry.

Stellar ages and masses for 23 stars were derived based on a comparison with PMS evolutionary tracks. 19 young stars are confirmed to be members of Serpens, while the remaining four could not be conclusively shown to have ages consistent with cluster membership. Six of these 19 confirmed stars show weak IR excess (below the Taurus median), while the other 13 are truly diskless sources.

We find that the age and mass distributions of this new diskless stellar population are remarkably similar to those of the disk-bearing young stars in the same region, studied previously by Oliveira et al. (2013).

This similarity may hold significant implications for the picture of disk evolution in which the main factors that determine disk fraction are mass and age. If confirmed for the larger sample of young diskless star candidates, our results indicate that other, yet poorly understood observationally, characteristics may play an important role as well.

This work is based on observations made with ESO Telescopes at Paranal Observatories under program ID 083.C-0766(B). The authors would like to thank the anonymous referee for her/his suggestions, that greatly improved this manuscript.

REFERENCES

- Alcalá, J. M., Spezzi, L., Chapman, N., et al. 2008, *ApJ*, 676, 427
- Alexander, R. D., Clarke, C. J., & Pringle, J. E. 2006, *MNRAS*, 369, 216
- Alexander, R. D., Clarke, C. J., & Pringle, J. E. 2006, *MNRAS*, 369, 229
- Allard, F., Hauschildt, P. H., & Schweitzer, A. 2000, *ApJ*, 539, 366
- Andrews, S. M., Rosenfeld, K. A., Kraus, A. L., & Wilner, D. J. 2013, *ApJ*, 771, 129
- Baraffe, I., Chabrier, G., Allard, F., & Hauschildt, P. 2001, *From Darkness to Light: Origin and Evolution of Young Stellar Clusters*, 243, 571

- Beccari, G., Spezzi, L., De Marchi, G., et al. 2010, *ApJ*, 720, 1108
- Carpenter, J. M., Mamajek, E. E., Hillenbrand, L. A., & Meyer, M. R. 2006, *ApJ*, 651, L49
- Cieza, L., Padgett, D. L., Stapelfeldt, K. R., et al. 2007, *ApJ*, 667, 308
- Clarke, C. J., Gendrin, A., & Sotomayor, M. 2001, *MNRAS*, 328, 485
- Dzib, S., Loinard, L., Mioduszewski, A. J., Boden, A. F., Rodríguez, L. F., & Torres, R. M. 2010, *ApJ*, 718, 610
- Ercolano, B., Clarke, C. J., & Drake, J. J. 2009, *ApJ*, 699, 1639
- Fang, M., van Boekel, R., Wang, W., et al. 2009, *A&A*, 504, 461
- Feigelson, E. D., & Kriss, G. A. 1981, *ApJ*, 248, L35
- Feigelson, E. D., & Montmerle, T. 1999, *ARA&A*, 37, 363
- Feigelson, E., Townsley, L., Güdel, M., & Stassun, K. 2007, *Protostars and Planets V*, 313
- Furlan, E., Hartmann, L., Calvet, N., et al. 2006, *ApJS*, 165, 568
- Getman, K. V., Feigelson, E. D., Grosso, N., et al. 2005, *ApJS*, 160, 353
- Gorti, U., Dullemond, C. P., & Hollenbach, D. 2009, *ApJ*, 705, 1237
- Güdel, M., Briggs, K. R., Arzner, K., et al. 2007, *A&A*, 468, 353
- Haisch, K. E., Jr., Lada, E. A., & Lada, C. J. 2001, *ApJ*, 553, L153
- Hartmann, L. 2003, *ApJ*, 585, 398
- Harvey, P. M., et al. 2006, *ApJ*, 644, 307
- Harvey, P. M., et al. 2007, *ApJ*, 663, 1139
- Harvey, P., Merín, B., Huard, T. L., Rebull, L. M., Chapman, N., Evans, N. J., II, & Myers, P. C. 2007, *ApJ*, 663, 1149
- Hauschildt, P. H., Allard, F., Ferguson, J., Baron, E., & Alexander, D. R. 1999, *ApJ*, 525, 871
- Hernández, J., Hartmann, L., Calvet, N., Jeffries, R. D., Gutermuth, R., Muzerolle, J., & Stauffer, J. 2008, *ApJ*, 686, 1195

- Hollenbach, D. J., Yorke, H. W., & Johnstone, D. 2000, *Protostars and Planets IV*, 401
- Evans, N. J., II, et al. 2007, delivery documentation¹
- Kennedy, G. M., & Kenyon, S. J. 2009, *ApJ*, 695, 1210
- Kenyon, S. J., & Hartmann, L. 1995, *ApJS*, 101, 117
- Kraus, A. L., Ireland, M. J., Hillenbrand, L. A., & Martinache, F. 2012, *ApJ*, 745, 19
- Luhman, K. L., Stauffer, J. R., Muench, A. A., et al. 2003, *ApJ*, 593, 1093
- Merín, B., Jørgensen, J., Spezzi, L., et al. 2008, *ApJS*, 177, 551
- Merín, B., et al. 2010, *ApJ*, 718, 1200
- Montes, D., Martin, E. L., Fernandez-Figueroa, M. J., Cornide, M., & de Castro, E. 1997, *A&AS*, 123, 473
- Mora, A., Merín, B., Solano, E., et al. 2001, *A&A*, 378, 116
- Mortier, A., Oliveira, I., & van Dishoeck, E. F. 2011, *MNRAS*, 418, 1194
- Muzerolle, J., Hillenbrand, L., Calvet, N., Briceño, C., & Hartmann, L. 2003, *ApJ*, 592, 266
- Natta, A., Testi, L., Muzerolle, J., et al. 2004, *A&A*, 424, 603
- Oliveira, I., et al. 2009, *ApJ*, 691, 672
- Oliveira, I., et al. 2010, *ApJ*, 714, 778
- Oliveira, I., Merín, B., Pontoppidan, K. M., & van Dishoeck, E. F. 2013, *ApJ*, 762, 128
- Owen, J. E., Ercolano, B., Clarke, C. J., & Alexander, R. D. 2010, *MNRAS*, 401, 1415
- Padgett, D. L., Cieza, L., Stapelfeldt, K. R., et al. 2006, *ApJ*, 645, 1283
- Pascucci, I., & Sterzik, M. 2009, *ApJ*, 702, 724
- Pascucci, I., Gorti, U., & Hollenbach, D. 2012, *ApJ*, 751, L42
- Preibisch, T., Kim, Y.-C., Favata, F., et al. 2005, *ApJS*, 160, 401

¹<http://ssc.spitzer.caltech.edu/legacy/c2dhistory.html>

- Randich, S., Pallavicini, R., Meola, G., Stauffer, J. R., & Balachandran, S. C. 2001, *A&A*, 372, 862
- Scelsi, L., Sacco, G., Affer, L., et al. 2008, *A&A*, 490, 601
- Sicilia-Aguilar, A., Henning, T., Dullemond, C. P., et al. 2011, *ApJ*, 742, 39
- Siess, L., Dufour, E., & Forestini, M. 2000, *A&A*, 358, 593
- Spezzi, L., Merín, B., Oliveira, I., van Dishoeck, E. F., & Brown, J. M. 2010, *A&A*, 513, A38
- Telleschi, A., Güdel, M., Briggs, K. R., Audard, M., & Scelsi, L. 2007, *A&A*, 468, 443
- van den Ancker, M. E., The, P. S., Feinstein, A., et al. 1997, *A&AS*, 123, 63
- Walter, F. M., & Kuhl, L. V. 1981, *ApJ*, 250, 254
- Walter, F. M., Brown, A., Mathieu, R. D., Myers, P. C., & Vrba, F. J. 1988, *AJ*, 96, 297
- Weingartner, J. C., & Draine, B. T. 2001, *ApJ*, 548, 296
- White, R. J., & Basri, G. 2003, *ApJ*, 582, 1109
- Winston, E., Megeath, S. T., Wolk, S. J., et al. 2007, *ApJ*, 669, 493
- Winston, E., Megeath, S. T., Wolk, S. J., et al. 2009, *AJ*, 137, 4777
- Winston, E., Megeath, S. T., Wolk, S. J., et al. 2010, *AJ*, 140, 266

Table 1. Observational log

Obs. Block ID	Field	Obs. night	Exp. time (s)
357791	Serpens AO5	11/Jun/2009	2000
357791	Serpens AO5	11/Jun/2009	2000
357792	Serpens AO5	11/Jun/2009	2000
357792	Serpens AO5	11/Jun/2009	2000
357792	Serpens AO5	11/Jun/2009	2000
357793	Serpens AO6	08/Jun/2009	2000
357793	Serpens AO6	08/Jun/2009	2000
365063	Serpens AO6	11/Jun/2009	2000
365063	Serpens AO6	11/Jun/2009	2000

Table 2. Observed objects in field AO5

ID ^a	RA (deg)	DEC (deg)	2MASS Name	R (mag)	Z (mag)	J (mag)	H (mag)	K (mag)	Good S/N?
03-005	277.39835	0.584499	18293563+0035035	18.2	14.3	12.0	10.8	10.3	Yes
03-007	277.29083	0.492694	18290985+0029329	19.2	15.6	12.4	10.8	10.1	No
03-008	277.24176	0.290611	18285808+0017243	21.9	18.0	10.7	9.8	9.4	No
03-009	277.25363	0.492055	18290088+0029312	17.0	14.1	11.6	10.0	9.0	Yes
03-011	277.37317	0.558027	18292959+0033280	20.8	16.0	13.7	12.6	12.1	No
03-012	277.37091	0.302722	18292905+0018091	17.2	14.7	12.4	11.4	10.9	Yes
03-013	277.28870	0.304611	18290934+0018159	22.4	18.3	14.4	12.0	11.0	No
03-014	277.27942	0.643972	18290698+0038378	21.9	18.0	15.2	12.9	11.5	No
03-015	277.43549	0.565333	18294460+0033553	19.4	15.7	12.7	11.9	11.5	No
03-017	277.34201	0.672361	18292209+0040203	23.0	17.4	13.3	11.1	10.0	Yes
03-020	277.26788	0.556611	18290437+0033235	21.9	18.0	15.9	13.0	11.3	No
03-021	277.35974	0.501416	18292641+0030043	21.9	18.0	16.2	13.9	12.9	No
03-022	277.25016	0.282972	18290025+0016578	17.7	15.2	12.9	11.5	10.7	No
03-023	277.32410	0.297277	18291770+0017488	21.9	18.0	13.3	12.7	12.4	No
03-025	277.40137	0.565749	18293634+0033559	21.4	16.3	13.8	12.3	11.6	No
03-026	277.28122	0.456777	18290748+0027234	17.0	14.7	13.2	12.6	12.3	Yes
03-027	277.31396	0.658166	18291521+0039343	20.4	16.1	13.4	12.1	11.5	Yes
03-028	277.17624	0.627361	18283136+0030534	21.9	18.0	14.4	13.0	12.3	No
03-029	277.27597	0.329388	18290615+0019442	18.8	15.6	13.4	12.2	11.8	No
03-030	277.43771	0.540333	18294516+0032245	20.3	16.6	13.2	11.9	11.3	No
03-032	277.24292	0.436444	18285828+0026103	17.8	15.5	14.0	13.4	13.2	Yes
03-033	277.31750	0.306361	18291617+0018222	21.0	18.0	14.3	11.8	10.1	No
03-034	277.13470	0.493916	–	21.9	18.0	–	–	–	No
03-035	277.26584	0.339027	18290394+0020212	15.6	13.7	11.6	10.1	9.1	No
03-037	277.43726	0.590944	18294502+0035264	21.6	18.3	14.1	12.3	11.4	No
03-038	277.12064	0.588888	18282871+0035206	19.8	16.8	14.2	13.0	12.5	No

^aAs in Brown et al., in prep.

Table 3. Observed objects in field AO6

ID ^a	RA (deg)	DEC (deg)	2MASS Name	R (mag)	Z (mag)	J (mag)	H (mag)	K (mag)	Good S/N?
02-002	277.50937	0.940555	18300227+0056259	13.5	12.3	10.8	10.1	9.9	Yes
02-004	277.34213	0.672472	18292209+0040203	23.0	17.4	13.3	11.1	10.0	No
02-005	277.43216	0.808805	18294372+0048308	15.8	14.7	13.3	12.6	12.5	Yes
02-006	277.22983	0.913722	18285512+0054496	19.7	16.7	14.2	13.0	12.6	No
02-007	277.18753	0.756916	18284499+0045239	16.6	14.0	11.9	10.8	10.4	Yes
02-008	277.51935	0.707138	18300459+0042247	16.2	14.3	12.5	11.5	11.2	Yes
02-009	277.31503	0.656249	18291564+0039227	21.1	17.0	14.1	12.8	12.1	No
02-010	277.54959	0.781416	18301185+0046519	17.0	15.2	13.4	12.5	12.1	No
02-013	277.47601	0.752222	18295424+0045074	13.5	11.9	10.4	9.8	9.5	Yes
02-014	277.52570	0.709277	18300616+0042336	14.2	12.3	9.8	8.6	7.5	Yes
02-017	277.21396	0.873749	18285134+0052270	16.1	13.5	11.9	11.3	11.0	No
02-019	277.45401	0.731916	–	–	–	–	–	–	No
02-021	277.22470	0.765194	18285396+0045528	18.7	15.7	13.3	12.1	11.5	No
02-022	277.35745	0.722611	–	–	–	–	–	–	No
02-024	277.35950	0.875499	–	–	–	–	–	–	No
02-025	277.56018	0.876055	18301440+0052352	17.0	15.2	12.5	11.6	11.2	Yes
02-027	277.50992	0.869249	18300236+0052098	17.6	15.1	13.1	12.0	11.6	Yes
02-028	277.45834	0.850444	18295003+0051014	18.0	15.3	13.0	11.9	11.4	Yes
02-029	277.42606	0.828666	18294221+0049431	19.5	16.5	14.0	12.8	12.3	Yes
02-030	277.48447	0.657055	18295628+0039246	17.0	15.2	13.1	12.1	11.7	No
02-031	277.42199	0.817277	18294122+0049020	19.3	16.2	13.8	12.5	11.9	No
02-033	277.28818	0.823861	–	–	–	–	–	–	No
02-036	277.25601	0.851166	–	21.2	18.8	–	–	–	No
02-037	277.44699	0.665388	18294727+0039555	17.0	15.2	13.6	12.6	12.1	Yes
02-038	277.46878	0.649944	–	–	–	–	–	–	No
02-039	277.41428	0.715833	18293946+0042570	18.6	16.6	13.6	12.4	11.9	Yes
02-041	277.43964	0.934277	18294546+0056026	19.6	16.4	13.5	12.1	11.4	No
02-043	277.26514	0.753805	18290362+0045135	19.9	16.4	13.5	12.1	11.6	Yes
02-047	277.35171	0.805138	–	–	–	–	–	–	No
02-048	277.30933	0.787027	18291396+0047165	20.8	17.8	15.1	13.8	13.4	No
02-049	277.40204	0.775999	18293650+0046333	19.5	16.2	13.5	12.2	11.7	Yes
02-050	277.28921	0.775749	18290943+0046343	18.1	15.3	13.3	12.2	11.8	No
02-051	277.55670	0.784777	18301365+0047055	17.0	15.2	13.2	12.3	12.0	Yes
02-052	277.48480	0.835527	–	–	–	–	–	–	No
02-053	277.51263	0.879194	18300298+0052460	19.8	16.8	14.5	13.7	13.2	No
02-054	277.35162	0.938861	18292426+0056189	17.6	14.8	12.5	11.5	11.1	No
02-055	277.34671	0.859694	–	–	–	–	–	–	No
02-056	277.24307	0.934805	18285837+0056050	20.4	16.6	14.1	13.1	12.6	No
02-057	277.40082	0.704499	18293620+0042163	18.8	16.6	13.3	11.9	11.3	Yes
02-058	277.30011	0.820249	–	22.7	20.4	–	–	–	No
02-059	277.26154	0.767055	–	–	–	–	–	–	No
02-060	277.20172	0.798305	18284840+0047515	17.2	15.1	13.2	12.2	11.9	No
02-061	277.53561	0.811666	–	22.2	19.2	–	–	–	No
02-062	277.35211	0.922777	–	–	–	–	–	–	No
02-063	277.38480	0.900916	18293237+0054024	18.0	15.6	13.5	12.5	12.1	Yes
02-064	277.45538	0.775388	–	–	–	–	–	–	No
02-065	277.47226	0.914527	18295337+0054523	19.7	16.7	14.0	12.7	12.1	No
02-068	277.34466	0.815555	18292277+0048569	19.5	16.6	14.0	12.8	12.4	No
02-069	277.40829	0.888111	18293799+0053154	22.7	18.9	15.6	14.3	13.7	No
02-072	277.53726	0.789472	18300893+0047219	17.7	15.4	13.5	12.4	12.0	Yes
02-073	277.27920	0.643722	18290698+0038378	17.0	15.2	15.2	12.9	11.5	No
02-074	277.42184	0.962361	–	22.3	19.6	–	–	–	No
02-076	277.35800	0.744583	18292588+0044396	20.4	16.2	13.7	12.5	12.2	No
02-079	277.39325	0.951666	–	–	–	–	–	–	No
02-080	277.44568	0.726527	18294682+0043396	17.0	15.2	15.7	13.6	12.7	No
02-081	277.39862	0.714861	18293575+0042499	22.8	19.0	15.5	14.2	13.5	No
02-083	277.46017	0.728611	18295042+0043435	17.8	15.4	13.0	11.5	10.5	No
02-086	277.40628	0.748555	–	–	–	–	–	–	No
02-088	277.38766	0.669555	18293301+0040087	17.0	15.2	14.5	12.9	12.0	No
02-093	277.44122	0.717305	–	–	–	–	–	–	No

^aAs in Brown et al., in prep.

Table 4. Spectral types of objects with classifiable spectra

Object ID	SpT	SpT range	H α ^a	Li ^a	IR excess?	X-ray Counts/s ^{b,c}	Log L _X (erg/s) ^b
03-005	M0	M0.5 – K0	strong E	A	Yes	0.0367(0.0303-0.0444)	30.05
03-009	M0.5	M2 – K7	strong E	A		0.0193(0.0151-0.0243)	29.62
03-012	M0	M2 – K2	weak E	A		0.0321(0.0244-0.0416)	29.95
03-017	K5	K7 – G7	A	–		0.0275(0.0207-0.0361)	29.79
03-026	M4	M6 – M2	weak E	–		0.0048(0.0018-0.0086)	29.09
03-027	G8	K5 – G0	A	–		0.0075(0.0049-0.0109)	29.47
03-032	M4	M6 – M2	weak E	–		0.0038(0.0007-0.0079)	28.86
02-002	K2	K7 – K0	A	A		0.0908(0.0845-0.0976)	30.35
02-005	M0	M0.5 – K5	weak E	–		0.0197(0.0175-0.0223)	29.70
02-007	M2	M3 – M0.5	weak E	A	Yes	0.0569(0.0508-0.0639)	30.10
02-008	K2	K7 – K0	–	A		0.0338(0.0299-0.0382)	29.90
02-013	G5	G8 – G2.5	A	A		0.0150(0.0127-0.0177)	29.52
02-014	G7	K0 – F0	weak E	A		0.0184(0.0154-0.0219)	29.60
02-025	G5	G8 – G2.5	A	–		0.0103(0.0084-0.0126)	29.84
02-027	M2	M3 – M0.5	weak E	A		0.0112(0.0091-0.0139)	29.41
02-028	M3	M4 – M0.5	weak E	A	Yes	0.0073(0.0058-0.0092)	29.29
02-029	M0	M0.5 – K7	weak E	A		0.0065(0.0051-0.0081)	29.20
02-037	M2	M3 – M0	strong E	A	Yes	0.0073(0.0053-0.0098)	29.27
02-039	K5	K7 – K0	–	A		0.0079(0.0062-0.0100)	29.32
02-043	M0.5	M3 – K7	weak E	A		0.0079(0.0060-0.0102)	29.24
02-049	M2	M3 – M0.5	weak E	A		0.0042(0.0030-0.0056)	28.92
02-051	M0.5	M2 – K7	weak E	A		0.0069(0.0049-0.0094)	29.27
02-057	K5	K7 – K0	A	A	Yes	0.0062(0.0046-0.0082)	29.13
02-063	M0.5	M3 – M0	weak E	A		0.0032(0.0020-0.0048)	28.92
02-072	M2	M3 – M0.5	strong E	A	Yes	0.0051(0.0034-0.0073)	29.11

^aE denotes emission and A denotes absorption

^bFrom Brown et al., in prep.

^cIn parenthesis is the 95% confidence range

Table 5. Stellar Parameters for the young diskless stars in Serpens

Object ID	Av (mag)	T_{eff} (K)	L_* (L_\odot)	Mass (M_\odot)	Age (Myr)
03-005	4.6	3850^{+1400}_{-65}	$1.52^{+1.22}_{-0.68}$	$1.06^{+0.18}_{-0.08}$	$1.01^{+20.31}_{-1.01}$
03-012	3.2	3850^{+1050}_{-290}	$0.73^{+0.58}_{-0.33}$	$0.98^{+0.06}_{-0.33}$	$3.06^{+27.13}_{-1.94}$
03-017	13.6	4350^{+1280}_{-290}	$5.87^{+4.72}_{-2.64}$	$1.60^{+0.12}_{-1.60}$	$1.00^{+6.74}_{-1.00}$
03-026	0.0	3270^{+290}_{-280}	$0.13^{+0.11}_{-0.06}$	$0.26^{+0.25}_{-0.15}$	$2.67^{+7.06}_{-2.67}$
03-032	0.0	3270^{+290}_{-280}	$0.06^{+0.05}_{-0.03}$	$0.23^{+0.27}_{-0.14}$	$6.83^{+23.38}_{-5.73}$
02-002	2.0	4900^{+350}_{-840}	$3.01^{+2.42}_{-1.35}$	$1.79^{+0.31}_{-1.10}$	$3.95^{+3.79}_{-3.95}$
02-005	0.0	3850^{+500}_{-65}	$0.13^{+0.11}_{-0.06}$	$0.73^{+0.09}_{-0.13}$	$30.71^{+47.73}_{-27.23}$
02-007	3.4	3560^{+225}_{-145}	$1.14^{+0.91}_{-0.51}$	$0.75^{+0.22}_{-0.13}$	$0.41^{+1.03}_{-0.41}$
02-008	4.0	4900^{+350}_{-840}	$1.09^{+0.87}_{-0.49}$	$1.18^{+0.00}_{-1.18}$	$20.16^{+22.94}_{-17.29}$
02-013	3.2	5770^{+75}_{-250}	$8.22^{+6.60}_{-3.69}$	$1.84^{+0.40}_{-0.35}$	$6.69^{+5.10}_{-2.55}$
02-014	10.3	5630^{+1570}_{-380}	$86.46^{+69.45}_{-38.86}$	$3.35^{+0.09}_{-0.09}$	$1.71^{+0.44}_{-0.44}$
02-025	5.1	5770^{+75}_{-250}	$1.92^{+1.54}_{-0.86}$	$1.35^{+0.01}_{-1.35}$	$24.50^{+980.15}_{-15.24}$
02-027	2.8	3560^{+225}_{-145}	$0.34^{+0.27}_{-0.15}$	$0.55^{+0.26}_{-0.13}$	$2.93^{+4.51}_{-1.42}$
02-028	3.5	3415^{+370}_{-145}	$0.40^{+0.32}_{-0.18}$	$0.45^{+0.38}_{-0.14}$	$1.44^{+4.56}_{-0.99}$
02-029	4.6	3850^{+210}_{-65}	$0.23^{+0.19}_{-0.11}$	$0.81^{+0.09}_{-0.09}$	$15.32^{+16.65}_{-8.32}$
02-037	2.8	3560^{+290}_{-145}	$0.21^{+0.17}_{-0.10}$	$0.53^{+0.27}_{-0.14}$	$5.68^{+11.80}_{-3.10}$
02-039	5.1	4350^{+900}_{-290}	$0.49^{+0.39}_{-0.22}$	$1.03^{+0.25}_{-0.18}$	$19.55^{+638.39}_{-11.23}$
02-043	5.4	3785^{+275}_{-370}	$0.47^{+0.38}_{-0.21}$	$0.85^{+0.20}_{-0.37}$	$4.71^{+4.98}_{-3.58}$
02-049	4.8	3560^{+225}_{-145}	$0.39^{+0.31}_{-0.17}$	$0.57^{+0.26}_{-0.12}$	$2.59^{+3.67}_{-1.38}$
02-051	1.9	3785^{+275}_{-225}	$0.25^{+0.20}_{-0.11}$	$0.78^{+0.07}_{-0.25}$	$10.36^{+15.54}_{-5.69}$
02-057	6.6	4350^{+900}_{-290}	$0.96^{+0.77}_{-0.43}$	$1.31^{+1}_{-1.31}$	$7.56^{+35.04}_{-4.61}$
02-063	3.0	3785^{+65}_{-370}	$0.24^{+0.19}_{-0.11}$	$0.78^{+0.06}_{-0.39}$	$10.67^{+15.66}_{-8.16}$
02-072	3.0	3650^{+135}_{-235}	$0.24^{+0.19}_{-0.11}$	$0.63^{+0.15}_{-0.23}$	$7.21^{+9.11}_{-4.65}$